Impact of Surface Charge Depletion on the Free Electron Nonlinear Response of Heavily Doped Semiconductors

Federico De Luca[1,2,*] and Cristian Ciracì[1,†]
[1]Istituto Italiano di Tecnologia, Center for Biomolecular Nanotechnologies, Via Barsanti 14, 73010 Arnesano, Italy
[2]Dipartimento di Matematica e Fisica "E. De Giorgi," Università del Salento, via Arnesano, 73100 Lecce, Italy

(Received 3 May 2022; accepted 26 August 2022; published 13 September 2022)

We propose surface modulation of the equilibrium charge density as a technique to control and enhance, via an external static potential, the free electron nonlinear response of heavily doped semiconductors. Within a hydrodynamic perturbative approach, we predict a 2 order of magnitude boost of free electron third-harmonic generation.

DOI: 10.1103/PhysRevLett.129.123902

Among the main challenges of modern applied physics, the control and the concentration of light at the subwavelength scale are of extreme importance for the realization of integrated optical technologies, especially to reach operational efficiencies in devices based on nonlinear optical effects, which otherwise would require high laser intensities and long propagation distances in macroscopic nonlinear crystals. Toward the accomplishment of this purpose, the study of the coupling of light with the collective oscillation of free electrons (FEs) in materials characterized by a high density of such carriers, i.e., plasmonics, has a central role. Plasmonic nanoantennas have been commonly used as local-field amplifiers in hybrid systems to enhance optical nonlinearity from dielectric material placed in their vicinity [1–4], however, the nonlinear response may also arise directly from the plasmonic material itself, specifically from the dynamics of nonequilibrium FEs [5–11]. Notoriously, noble metals are the main constituents of plasmonic devices in the visible spectrum. On the other hand, heavily doped semiconductors (i.e., with charge densities $n_0 \sim 10^{19} - 10^{20}$ cm^{-3}) have emerged as alternative materials for plasmonics in the near-infrared (NIR), i.e., $0.8 < \lambda < 2$ μm, and in the mid-infrared (MIR), i.e., $2 < \lambda < 20$ μm [12–16]. Being low-loss high-quality materials that can be compatible with standard microelectronics fabrication processes, and being their optical response tunable through electrical or optical doping, heavily doped semiconductors offer a unique perspective for integrated optical devices in the NIR and in the MIR [17–20].

Within this context, we have recently investigated the FE nonlinear optical dynamics of heavily doped semiconductors, predicting that cascaded third-harmonic generation (THG) due to second-harmonic signals can be as strong as direct THG contributions, even when the second-harmonic generation efficiency is zero, and showing that, when coupled with plasmonic enhancement, FE nonlinearities could be up to 2 orders of magnitude larger than conventional semiconductor nonlinearities [21,22]. We employed a hydrodynamic description that includes terms up to the third order, usually negligible for noble metals. This choice has been made taking into consideration that, within the hydrodynamic formalism, the third-order response, expressed through the third-order polarization vector $\mathbf{P}_{\mathrm{NL}}^{(3)}$, is inversely proportional to the squared equilibrium charge density, i.e., $\mathbf{P}_{\mathrm{NL}}^{(3)} \propto (1/n_0^2)$. Indeed, doped semiconductors with a plasma wavelength in the MIR have a charge density ($n_0 \sim 10^{19}$ cm^{-3}) much lower than noble metals, such as gold ($n_0 \sim 10^{22}$ cm^{-3}). Hence, FE nonlinearites may grow as much as 6 orders of magnitude, overcoming by far the contributions originating in the crystal lattice nonlinear susceptibility $\chi^{(3)}$, which instead represents the dominant third-order nonlinear source in gold due to the high concentration of charge carriers. Moreover, the nonlinear active volumes are expected to increase in semiconductors due to their smaller effective masses [21].

A further step forward along this direction can be made if another very important characteristic of hydrodynamic nonlinearities is considered: they emerge predominantly at the surface [23,24]. As a consequence, an induced decrease of the electron density, in a small region of the semiconductor very close to its surface, may be exploited to increase the nonlinear response strength of the plasmonic system. In doped semiconductors, such a modification of the charge density can be obtained through the application of an external bias, i.e., by means of field-effect modulation [25–31]. Therefore, this technique may provide the unique ability to externally and dynamically modulate the nonlinear coefficients of heavily doped semiconductors by a simple setting of dc electric potential levels. In this Letter we present a model for describing the influence of surface charge depletion on FE nonlinearities and make quantitative predictions about the role of field-effect modulation for the control of the optical nonlinear response of heavily doped semiconductors. Finally, we demonstrate a 2 order of magnitude enhancement in THG from a doped InP grating

resonant in the MIR, considering an external bias of the order of 100 V/μm.

As in our previous works on FE nonlinearities [21,22], for the representation of nonlinear and nonlocal FE dynamics, we apply the quasiclassical formalism of the hydrodynamic model in the limit of Thomas-Fermi approximation [32–34]. Within this framework, the following constitutive relation is employed to model the FE fluid via two macroscopic variables, its charge density $n(\mathbf{r},t)$, and its current density $\mathbf{J}(\mathbf{r},t)=-en\mathbf{v}$, with $\mathbf{v}(\mathbf{r},t)$ being the electron velocity field

$$\dot{\mathbf{J}}+\gamma\mathbf{J}=\frac{e^2n}{m}\mathbf{E}-\frac{\mu_0 e}{m}\mathbf{J}\times\mathbf{H}+\frac{1}{e}\left(\frac{\mathbf{J}}{n}\nabla\cdot\mathbf{J}+\mathbf{J}\cdot\nabla\frac{\mathbf{J}}{n}\right)+\frac{en}{m}\nabla\frac{\delta T[n]}{\delta n}, \quad (1)$$

where time derivatives are expressed in dot notation, m is the electron effective mass, e the elementary charge (in absolute value), μ_0 is the magnetic permeability of vacuum, and γ is the damping rate. This equation portrays the many-body nonlinear dynamics of the charge carriers under the influence of external electric $\mathbf{E}(\mathbf{r},t)$ and magnetic $\mathbf{H}(\mathbf{r},t)$ fields. Furthermore, the fermionic nature of FEs, which cannot be compressed in an infinitesimally thin layer, is accounted by means of the electron pressure term, where $T[n]$, is the kinetic energy functional. On the other hand, we neglect electron spill-out and apply hard-wall boundary conditions.

Employing a perturbative approach, we can write the charge density as a sum of a static and a dynamic term:

$$n(\mathbf{r},t)=n_0(\mathbf{r})+n_d(\mathbf{r},t), \quad (2)$$

where $n_0(\mathbf{r})$ is the equilibrium state nonperturbed electron charge density and $n_d\ll n_0$ is the induced charge density, representing perturbative corrections to the equilibrium density. Similarly, the electric field and the kinetic functional can be written as $\mathbf{E}(\mathbf{r},t)=\mathbf{E}_0(\mathbf{r})+\mathbf{E}_d(\mathbf{r},t)$ and $T[n](\mathbf{r},t)=T_0[n_0(\mathbf{r})]+T_d[n(\mathbf{r},t)]$, respectively. As a consequence, Eq. (1) can be split into a static and a dynamic equation:

$$\nabla\frac{\delta T_0[n_0]}{\delta n_0}+e\mathbf{E}_0=0 \quad (3a)$$

$$\dot{\mathbf{J}}+\gamma\mathbf{J}=\frac{e^2n}{m}\mathbf{E}_d-\frac{\mu_0 e}{m}\mathbf{J}\times\mathbf{H}+\frac{1}{e}\left(\frac{\mathbf{J}}{n}\nabla\cdot\mathbf{J}+\mathbf{J}\cdot\nabla\frac{\mathbf{J}}{n}\right)+\frac{en}{m}\nabla\frac{\delta T_d[n]}{\delta n}. \quad (3b)$$

Equation (3a) coupled to the Poisson equation would give a self-consistent expression for the equilibrium density and the static electric field. However, we calculate $n_0(\mathbf{r})$ by means of the method described in the Supplemental Material [35], which takes into account bands bending in doped semiconductors within the parabolic band approximation [30,31,36]. Note that this method is equivalent to solving Eq. (3a) for a proper expression of the static kinetic functional $T_0[n_0]$. To solve the dynamic Eq. (3b), we consider the kinetic energy functional within the Thomas-Fermi approximation, i.e., $(\delta T_d[n]/\delta n)=\frac{5}{3}c_{\mathrm{TF}}(n^{\frac{2}{3}}-n_0^{\frac{2}{3}})$, with $c_{\mathrm{TF}}=(\hbar^2/m)(3/10)(3\pi^2)^{2/3}$. Considering a Taylor expansion up to the third order, we can rewrite $n^{\frac{2}{3}}-n_0^{\frac{2}{3}}=n_0^{2/3}[\frac{2}{3}(n_d/n_0)-\frac{1}{9}(n_d/n_0)^2+(4/81)(n_d/n_0)^3]$ such that, after some algebra, the quantum pressure term becomes

$$\frac{en}{m}\nabla\frac{\delta T_d[n]}{\delta n}\simeq e\beta^2\left[1+\frac{2}{3}\frac{n_d}{n_0}-\frac{1}{9}\left(\frac{n_d}{n_0}\right)^2\right]\nabla n_d+e\beta^2\left[-\frac{1}{3}\frac{n_d}{n_0}-\frac{1}{9}\left(\frac{n_d}{n_0}\right)^2+\frac{4}{81}\left(\frac{n_d}{n_0}\right)^3\right]\nabla n_0, \quad (4)$$

where $\beta(\mathbf{r})^2=(10/9)(c_{\mathrm{TF}}/m)n_0(\mathbf{r})^{2/3}$. Equation (3b) can be then written in terms of the polarization field $\mathbf{P}(\mathbf{r},t)$, with $\dot{\mathbf{P}}=\mathbf{J}$, $n_d=(1/e)\nabla\cdot\mathbf{P}$, and $n^{-1}\simeq n_0^{-1}[1-(n_d/n_0)]$, as

$$\ddot{\mathbf{P}}+\gamma\dot{\mathbf{P}}=\frac{n_0e^2}{m}\mathbf{E}+\beta^2\nabla(\nabla\cdot\mathbf{P})-\frac{1}{3}\frac{\beta^2}{n_0}(\nabla\cdot\mathbf{P})\nabla n_0+\mathbf{S}_{\mathrm{NL}}, \quad (5)$$

where $\mathbf{S}_{\mathrm{NL}}=\mathbf{S}_{\mathrm{NL}}^{(2)}+\mathbf{S}_{\mathrm{NL}}^{(3)}$ includes second- and third-order nonlinear sources, respectively:

$$\mathbf{S}_{\mathrm{NL}}^{(2)}=\frac{e}{m}\mathbf{E}\nabla\cdot\mathbf{P}-\frac{e\mu_0}{m}\dot{\mathbf{P}}\times\mathbf{H}+\frac{1}{en_0}(\dot{\mathbf{P}}\nabla\cdot\dot{\mathbf{P}}+\dot{\mathbf{P}}\cdot\nabla\dot{\mathbf{P}})-\frac{1}{en_0^2}\dot{\mathbf{P}}(\dot{\mathbf{P}}\cdot\nabla n_0)+\frac{1}{3}\frac{\beta^2}{en_0}\nabla(\nabla\cdot\mathbf{P})^2-\frac{1}{9}\frac{\beta^2}{en_0^2}(\nabla\cdot\mathbf{P})^2\nabla n_0, \quad (6a)$$

$$\mathbf{S}_{\mathrm{NL}}^{(3)}=-\frac{1}{e^2n_0^2}[\nabla\cdot\mathbf{P}(\dot{\mathbf{P}}\nabla\cdot\dot{\mathbf{P}}+\dot{\mathbf{P}}\cdot\nabla\dot{\mathbf{P}})+\dot{\mathbf{P}}\cdot\dot{\mathbf{P}}\nabla\nabla\cdot\mathbf{P}]+\frac{2}{e^2n_0^3}(\nabla\cdot\mathbf{P})\dot{\mathbf{P}}(\dot{\mathbf{P}}\cdot\nabla n_0)-\frac{1}{27}\frac{\beta^2}{e^2n_0^2}\nabla(\nabla\cdot\mathbf{P})^3+\frac{4}{81}\frac{\beta^2}{e^2n_0^3}(\nabla\cdot\mathbf{P})^3\nabla n_0. \quad (6b)$$

A development with respect to previous works [5,6,21] is represented by the introduction of nonlinear contributions proportional to ∇n_0, by means of which we tackle the nonzero gradient of the equilibrium density. In any case, due to constructive interference between the nonlinear sources in the near and far field [24], it is not straightforward to make clear comparisons of the contributions and define

the dominant one. The aforementioned new terms and all the surface contributions, i.e., those proportional to $\nabla \cdot \mathbf{P}$, describe nonlinear effects whose origin is at the surface of the material. Consequently, hydrodynamic nonlinearities are expected to be extremely sensitive to the changes of the physical condition at the surface, such as a change in the density n_0.

At this point, if a time-harmonic dependence of the fields is assumed, i.e., $\mathbf{F}(\mathbf{r}, t) = \sum_j \mathbf{F}_j(\mathbf{r}) e^{-i\omega_j t}$, with $\mathbf{F} = \mathbf{E}$, $\mathbf{H}$, or $\mathbf{P}$, combining Eqs. (5) and (6) with Maxwell's equations, the following system can be derived for each harmonic ω_j:

$$\nabla \times \nabla \times \mathbf{E}_j - \varepsilon \frac{\omega_j^2}{c^2} \mathbf{E}_j - \omega_i^2 \mu_0 (\mathbf{P}_j + \mathbf{P}_{\omega_j}^{\mathrm{NL}}) = 0, \tag{7a}$$

$$\beta^2 \nabla(\nabla \cdot \mathbf{P}_j) - \frac{1}{3} \frac{\beta^2}{n_0} (\nabla \cdot \mathbf{P}_j) \nabla n_0 + (\omega^2 + i\gamma\omega) \mathbf{P}_j = -\frac{n_0 e^2}{m} \mathbf{E}_j + \mathbf{S}_{\omega_j}, \tag{7b}$$

where local contributions from the semiconductor, both linear, through the local permittivity ε, and nonlinear, through the nonlinear polarization $\mathbf{P}_{\omega_j}^{\mathrm{NL}}$ are considered. Since a coupling between different harmonics occurs through the nonlinear contributions $\mathbf{P}_{\omega_j}^{\mathrm{NL}}$ and $\mathbf{S}_{\omega_j}$, Eqs. (7) constitute a set of coupled nonlinear differential equations, whose resolution is not straightforward. For this reason, as we expect harmonic signals to be several orders of magnitude smaller than the pump fields, we assume that the latter is not affected by the nonlinear process (undepleted pump approximation), i.e., $\mathbf{P}_{\omega_1}^{\mathrm{NL}} = \mathbf{S}_{\omega_1} = 0$. The system of Eqs. (7) reduces then to separated sets of one-way coupled equations, one for each harmonic. Moreover, since our goal is to study the impact of surface depletion on FE nonlinearities, we neglect contribution from the background lattice, i.e., $\mathbf{P}_{\omega_3}^{\mathrm{NL}} = 0$. Indeed, we have shown [21] that FE nonlinearities may be larger than those coming from the bulk $\chi^{(3)}$, especially when the fundamental field (FF) wavelength is deep in the metallic region of the semiconductor and for high angles of incidence, even without surface charge modulation. As a consequence, being the application of a static electric field very favorable for hydrodynamic nonlinearities, it is safe to concentrate the analysis on these contributions. In what follows, we focus on direct FE THG, i.e., a third-order process where three photons of energy $\hbar\omega$ combine to give a single photon of energy $3\hbar\omega$, while we briefly discuss cascaded FE THG in the Supplemental Material [35], where we report also the expressions of the nonlinear sources, $\mathbf{S}_{\omega_j}$, derived from Eqs. (6).

In order to estimate the impact of surface charge depletion on the FE nonlinear response of heavily doped semiconductors, we first apply the developed formalism to calculate the FE THG efficiency η of a semiconductor slab. In particular, we solved Eqs. (7) numerically using the finite-elements method within a customized frequency-dependent two-dimensional implementation in COMSOL Multiphysics [37]. The efficiency has been calculated by normalizing the power of the generated signal to the input power at the fundamental frequency, $\eta = I_G/I_0$, where I_G is the generated intensity. As a consequence, for third-order nonlinearities, η will scale with I_0^2.

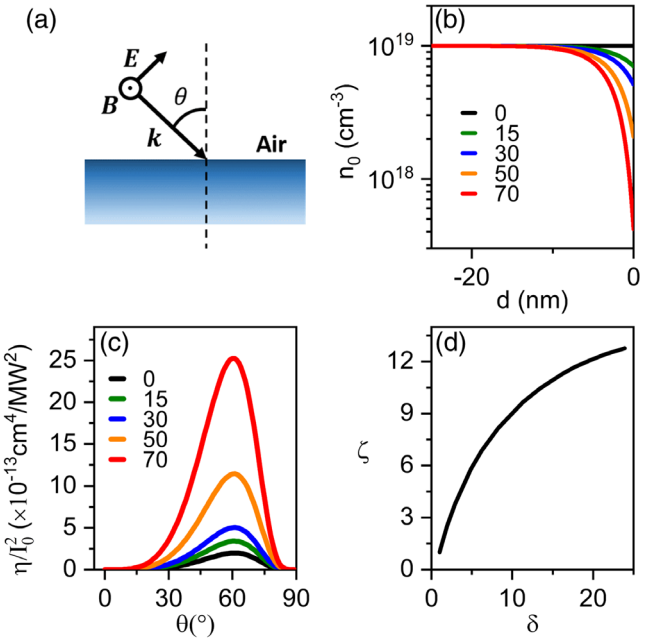

FIG. 1. Effects of surface charge depletion on the FE THG efficiency η of a doped InP slab: (a) a TM plane wave impinging on a semi-infinite geometry is considered; (b) equilibrium charge density $n_0(\mathbf{r})$ as a function of the distance d from the surface of the slab for different levels of modulation (in V/μm); (c) related η, normalized to the squared input intensity I_0^2, as a function of the angle of incidence θ; (d) enhancement factors ζ as a function of the depletion factor δ in correspondence of the peak efficiencies at $\theta = 60$.

To accurately model the semiconductor's linear response, on top of the Drude-like dispersion described by Eq. (5), we consider a local permittivity contribution, ε_∞, such that, neglecting nonlocal effects, we retrieve the usual dielectric function $\varepsilon(\omega) = \varepsilon_\infty - [\omega_P^2/(\omega^2 + i\gamma\omega)]$, where $\omega_P = \sqrt{[e^2 n_0/(\varepsilon_0 m)]}$ is the plasma frequency of the semiconductor, being ε_0 the dielectric constant of vacuum. The input field is a TM plane wave impinging on the geometry with a certain angle of incidence θ [see Fig. 1(a)]. The slab is characterized by an equilibrium charge density profile modulated in a very small region at the top interface, as shown by the curves in Fig. 1(b), calculated assuming the electric potential on the surface of the semiconductor, as described in the Supplemental Material [35]. The imposed boundary conditions on the top surface of the semiconductor slab correspond to an applied static electric field that can be up to 70 V/μm.

The material considered for this Letter is indium phosphide (InP), a direct band gap III-V semiconductor and a low loss plasmonic material for the MIR region [19,38,39]. InP is, thanks to its intrinsic properties ($m = 0.078\ m_e$, $\varepsilon_\infty = 9.55$ [19]), among the most promising semiconductors for the realization of integrated optical platforms based on FE nonlinear dynamics [22]. Since we assume the value of the equilibrium charge density in the bulk to be $n_b = 10^{19}$ cm^{-3}, the simulated InP's slab has a screened plasma wavelength in the MIR, $\tilde{\lambda}_p = 9.1\ \mu$m, where $\tilde{\lambda}_p = (2\pi c/\tilde{\omega}_p)$, with $\tilde{\omega}_p = \omega_p/\sqrt{\varepsilon_\infty}$ being the screened plasma frequency. Finally, $\gamma = 1$ ps^{-1} has been assumed dispersion-less [21]. Note that, given the dimension of the system, the effects of the depletion region on the linear properties of the semiconductor are not sensitive.

In Fig. 1(c), we report η of FE THG, normalized to the squared input intensity I_0^2, as a function of θ for the five different $n_0(\mathbf{r})$ profiles of plot b, at a FF wavelength $\lambda_{\mathrm{FF}} = 12\ \mu$m, while, in Fig. 1(d), we show its enhancement factor $\zeta = \eta/\eta_0$ (where η_0 is the THG efficiency obtained with no applied potential) in correspondence of the peak efficiencies (i.e., for $\theta = 60°$), as a function of the depletion factor $\delta = n_b/n_0^{\mathrm{surf}}$, where n_0^{surf} is the value of n_0 for $d = 0$. Here, the angular dispersion of η is typical of third-order FE THG, i.e., it is null at normal incidence and grows with θ, peaking at a high angle of incidence. The reason is that, for $\theta = 0°$, the electric field is parallel to the slab; as a result there cannot be charge oscillations of the charge carriers in the finite dimension of the slab [21]. Instead, the important feature emerging from Fig. 1 is the boost of FE THG because of the localized diminution of $n_0(\mathbf{r})$ in a very thin region (∼10 nm) in proximity of the surface of the doped semiconductor. Indeed, as it can be observed more clearly in Fig. 1(d), the enhancement factor of THG can be larger than 1 order of magnitude for $\delta \approx 25$, i.e., for n_0^{surf} about 25 times smaller than n_b.

As a next step, it may be interesting to employ our hydrodynamic formalism with the aim of studying the possible impact of charge depletion on the nonlinear response of a nanopatterned semiconductor slab characterized by a localized plasmon resonance in the MIR. We consider an infinite array of subwavelength grooves (a grating) portrayed in Fig. 2(a), a structure that supports plasmonic resonances and allows us to couple virtually all incident energy into the active material at normal incidence and locally enhance the pump field [40], and, as a consequence, to have nonzero FE THG already for $\theta = 0°$. The pattern has been designed as a function of the parameter a, h, and d, in order to be resonant in the MIR for a TM-polarized excitation, obtaining a resonance around $\lambda_{\mathrm{FF}} = 12.2\ \mu$m, i.e., where the reflectance is almost zero. The doped semiconductor and the boundary conditions are the same considered for the simple slab. The difference is that now the region of charge depletion follows the contour of the grooves,

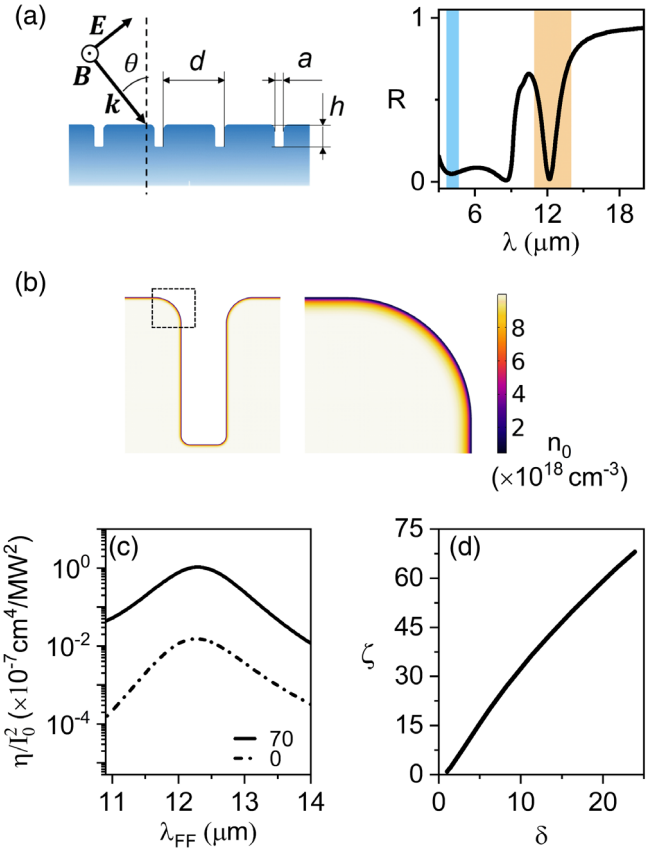

FIG. 2. Effects of surface charge depletion on the FE THG efficiency η of a doped InP semi-infinite grating: (a) the structure and its reflectance R at normal incidence for $n_b = 10^{19}$ cm^{-3}, $d = 1\ \mu$m, $a = 150$ nm, $h = 500$ nm. The orange and the light blue shadows evidence the considered range of variation of λ_{FF} and that of the corresponding λ_{TH}, respectively. (b) $n_0(\mathbf{r})$ along the grooves contour in the case of maximum depletion of Fig. 1(b); (c) normalized efficiencies of THG as a function of λ_{FF} in the proximity of the resonance, at normal incidence, in the case of zero and maximum modulation (in V/μm); (d) related enhancement factors ζ as a function of the depletion factor δ in correspondence of the peak efficiencies at $\lambda_{\mathrm{FF}} = 12.2\ \mu$m.

as depicted in Fig. 2(b). To study the nonlinear properties of the grating, we report in Fig. 2(c) the normalized efficiencies of FE THG, in this case as a function of λ_{FF}, in proximity of the resonance and at normal incidence, showing a comparison of the undepleted case with that of maximum modulation. In all cases, the maximum efficiency reached is about 5 orders of magnitude larger that obtained for the simple slab. Finally, in Fig. 2(d), we portray ζ in correspondence of the peak efficiencies of plot (c), as a function of the depletion factor. Here, an enhancement of the efficiency when the depth of the region of depletion increases can be put in evidence also for the grating. Nevertheless, in Fig. 2(d), ζ is in all cases larger if compared to the same points in Fig. 1(d), reaching $\zeta \approx 70$. The peak efficiency of direct THG is larger than 10^{-5} if an input intensity of 10 MW/cm^2 is assumed.

In conclusion, in order to evaluate the impact of surface charge depletion on the FE nonlinear response of heavily doped semiconductors, we have introduced a hydrodynamic perturbative approach that takes into account the nonzero gradient of $n_0(\mathbf{r})$. We have employed our method to study THG in a simple slab and in a resonant grating of doped InP, showing a boost of the efficiency of generation caused by the localized diminution of $n_0(\mathbf{r})$ on the surface of the material, and predicting an enhancement of the THG up to 2 orders of magnitude with an applied external static bias of 70 V/μm. Our Letter highlights the role of field-effect gated modulation as a ground-breaking tool to externally and dynamically control the nonlinear coefficients of heavily doped semiconductors, opening a new route toward the development of integrated nonlinear optics at MIR frequencies.

*federico.deluca@iit.it
†cristian.ciraci@iit.it

[1] J. Deng, Y. Tang, S. Chen, K. Li, A. V. Zayats, and G. Li, Giant enhancement of second-order nonlinearity of epsilon-near- zero medium by a plasmonic metasurface, Nano Lett. **20**, 5421 (2020).
[2] Q. Shen, W. Jin, G. Yang, A. W. Rodriguez, and M. H. Mikkelsen, Active control of multiple, simultaneous nonlinear optical processes in plasmonic nanogap cavities, ACS Photonics **7**, 901 (2020).
[3] A. Noor, A. R. Damodaran, I.-H. Lee, S. A. Maier, S.-H. Oh, and C. Ciracì, Mode-matching enhancement of second-harmonic generation with plasmonic nanopatch antennas, ACS Photonics **7**, 3333 (2020).
[4] R. Sarma, D. d. Ceglia, N. Nookala, M. A. Vincenti, S. Campione, O. Wolf, M. Scalora, M. B. Sinclair, M. A. Belkin, and I. Brener, Broadband and efficient second-harmonic generation from a hybrid dielectric metasurface/semiconductor quantum-well structure, ACS Photonics **6**, 1458 (2019).
[5] M. Scalora, M. A. Vincenti, D. de Ceglia, V. Roppo, M. Centini, N. Akozbek, and M. J. Bloemer, Second- and third-harmonic generation in metal-based structures, Phys. Rev. A **82**, 043828 (2010).
[6] C. Ciracì, E. Poutrina, M. Scalora, and D. R. Smith, Origin of second-harmonic generation enhancement in optical split-ring resonators, Phys. Rev. B **85**, 201403(R) (2012).
[7] M. Kauranen and A. V. Zayats, Nonlinear plasmonics, Nat. Photonics **6**, 737 (2012).
[8] A. V. Krasavin, P. Ginzburg, and A. V. Zayats, Free-electron optical nonlinearities in plasmonic nanostructures: A review of the hydrodynamic description, Laser Photonics Rev. **12**, 1700082 (2018).
[9] F. De Luca and C. Ciracì, Difference-frequency generation in plasmonic nanostructures: A parameter-free hydrodynamic description, J. Opt. Soc. Am. B **36**, 1979 (2019).
[10] L. Rodríguez-Suné, M. Scalora, A. S. Johnson, C. Cojocaru, N. Akozbek, Z. J. Coppens, D. Perez-Salinas, S. Wall, and J. Trull, Study of second and third harmonic generation from an indium tin oxide nanolayer: Influence of nonlocal effects and hot electrons, APL Photonics **5**, 010801 (2020).
[11] A. Noor, M. Khalid, F. De Luca, H. M. Baghramyan, M. Castriotta, A. D'Orazio, and C. Ciracì, Second-harmonic generation in plasmonic waveguides with nonlocal response and electron spill-out, Phys. Rev. B **106**, 045415 (2022).
[12] J. Frigerio *et al.*, Tunability of the dielectric function of heavily doped germanium thin films for mid-infrared plasmonics, Phys. Rev. B **94**, 085202 (2016).
[13] J. R. Maack, N. A. Mortensen, and M. Wubs, Size-dependent nonlocal effects in plasmonic semiconductor particles, Europhys. Lett. **119**, 17003 (2017).
[14] M. P. Fischer, A. Riede, K. Gallacher, J. Frigerio, G. Pellegrini, M. Ortolani, D. J. Paul, G. Isella, A. Leitenstorfer, P. Biagioni, and D. Brida, Plasmonic mid-infrared third harmonic generation in germanium nanoantennas, Light. Sci. Appl. **7**, 106 (2018).
[15] M. P. Fischer, N. Maccaferri, K. Gallacher, J. Frigerio, G. Pellegrini, D. J. Paul, G. Isella, A. Leitenstorfer, P. Biagioni, and D. Brida, Field-resolved detection of the temporal response of a single plasmonic antenna in the mid-infrared, Optica **8**, 898 (2021).
[16] C. A. Chavarin, E. Hardt, S. Gruessing, O. Skibitzki, I. Costina, D. Spirito, W. Seifert, W. Klesse, C. L. Manganelli, C. You, J. Flesch, J. Piehler, M. Missori, L. Baldassarre, B. Witzigmann, and G. Capellini, n-type Ge/Si antennas for THz sensing, Opt. Express **29**, 7680 (2021).
[17] R. Soref, Mid-infrared photonics in silicon and germanium, Nat. Photonics **4**, 495 (2010).
[18] A. Boltasseva and H. A. Atwater, Low-loss plasmonic metamaterials, Science **331**, 290 (2011).
[19] G. V. Naik, V. M. Shalaev, and A. Boltasseva, Alternative plasmonic materials: Beyond gold and silver, Adv. Mater. **25**, 3264 (2013).
[20] T. Taliercio and P. Biagioni, Semiconductor infrared plasmonics, Nanophotonics **8**, 949 (2019).
[21] F. De Luca, M. Ortolani, and C. Ciracì, Free electron nonlinearities in heavily doped semiconductors plasmonics, Phys. Rev. B **103**, 115305 (2021).
[22] F. De Luca, M. Ortolani, and C. Ciracì, Free electron harmonic generation in heavily doped semiconductors: The role of the materials properties, Eur. Phys. J. Appl. Metamater. **9**, 13 (2022).
[23] J. E. Sipe, V. C. Y. So, M. Fukui, and G. I. Stegeman, Analysis of second-harmonic generation at metal surfaces, Phys. Rev. B **21**, 4389 (1980).
[24] C. Ciracì, E. Poutrina, M. Scalora, and D. R. Smith, Second-harmonic generation in metallic nanoparticles: Clarification of the role of the surface, Phys. Rev. B **86**, 115451 (2012).
[25] N. Bloembergen and P. Pershan, Light waves at the boundary of nonlinear media, Phys. Rev. **128**, 606 (1962).
[26] R. Terhune, P. Maker, and C. Savage, Optical Harmonic Generation in Calcite, Phys. Rev. Lett. **8**, 404 (1962).
[27] C. Lee, R. Chang, and N. Bloembergen, Nonlinear Electroreflectance in Silicon and Silver, Phys. Rev. Lett. **18**, 167 (1967).
[28] P. G. Dzhavakhidze, A. A. Kornyshev, A. Liebsch, and M. Urbakh, Theory of second-harmonic generation at the metal-electrolyte interface, Phys. Rev. B **45**, 9339 (1992).

[29] S. Chen, K. F. Li, G. Li, K. W. Cheah, and S. Zhang, Gigantic electric-field-induced second harmonic generation from an organic conjugated polymer enhanced by a band-edge effect, Light. Sci. Appl. **8**, 17 (2019).
[30] O. Zandi, A. Agrawal, A. B. Shearer, L. C. Reimnitz, C. J. Dahlman, C. M. Staller, and D. J. Milliron, Impacts of surface depletion on the plasmonic properties of doped semiconductor nanocrystals, Nat. Mater. **17**, 710 (2018).
[31] M. Ghini, N. Curreli, M. B. Lodi, N. Petrini, M. Wang, M. Prato, A. Fanti, L. Manna, and I. Kriegel, Control of electronic band profiles through depletion layer engineering in core–shell nanocrystals, Nat. Commun. **13**, 1 (2022).
[32] C. Ciracì, J. B. Pendry, and D. R. Smith, Hydrodynamic model for plasmonics: A macroscopic approach to a microscopic problem, ChemPhysChem **14**, 1109 (2013).
[33] C. Ciracì, Current-dependent potential for nonlocal absorption in quantum hydrodynamic theory, Phys. Rev. B **95**, 245434 (2017).
[34] C. Ciracì and F. Della Sala, Quantum hydrodynamic theory for plasmonics: Impact of the electron density tail, Phys. Rev. B **93**, 205405 (2016).
[35] See Supplemental Material at http://link.aps.org/supplemental/10.1103/PhysRevLett.129.123902 for the derivation of the surface depleted equilibrium charge density, the hydrodynamic nonlinear sources for THG, and a comment about the impact of surface charge depletion on cascaded THG.
[36] R. Seiwatz and M. Green, Space charge calculations for semiconductors, J. Appl. Phys. **29**, 1034 (1958).
[37] COMSOL Multiphysics, www.comsol.com.
[38] M. E. A. Panah, O. Takayama, S. V. Morozov, K. E. Kudryavtsev, E. S. Semenova, and A. V. Lavrinenko, Highly doped InP as a low loss plasmonic material for mid-IR region, Opt. Express **24**, 29077 (2016).
[39] M. E. A. Panah, L. Han, K. Norrman, N. Pryds, A. Nadtochiy, A. Zhukov, A. V. Lavrinenko, and E. S. Semenova, Mid-IR optical properties of silicon doped InP, Opt. Mater. Express **7**, 2260 (2017).
[40] M. Dechaux, P. H. Tichit, C. Ciracì, J. Benedicto, R. Pollès, E. Centeno, D. R. Smith, and A. Moreau, Influence of spatial dispersion in metals on the optical response of deeply subwavelength slit arrays, Phys. Rev. B **93**, 045413 (2016).